Build Simul (2024) 17: 1273–1287
https://doi.org/10.1007/s12273-024-1138-1

Generic load regulation strategy for enhancing energy efficiency of chiller plants

Hang Wan[1], Yuyang Gong[1], Shengwei Wang[2], Yongjun Sun[1], Tao Xu[3], Gongsheng Huang[1,4] (✉)

1. Department of Architecture and Civil Engineering, City University of Hong Kong, Hong Kong, China
2. Department of Building Environment and Energy Engineering, Hong Kong Polytechnic University, Hong Kong, China
3. School of Civil Engineering, Guangzhou University, Guangzhou, China
4. Shenzhen Research Institute of City University of Hong Kong, Shenzhen, China

Abstract

In many chiller plants, high coefficient of performance (COP) is only achieved at a few favorable part load ratios (PLRs), while the COP is low at many other non-favorable PLRs. To address this issue, this study proposes a generic load regulation strategy that aims to maintain chiller plants operating at high COP, particularly under non-favorable PLRs. This is achieved by incorporating thermal energy storage (TES) units and timely optimizing the charging and discharging power of the integrated TES units. The optimal charging and discharging power is determined by solving a dynamic optimization problem, taking into account the performance constraints of the TES units and the chiller plants. To provide an overview of the energy-saving potential of the proposed strategy, a comprehensive analysis was conducted, considering factors such as building load profiles, COP/PLR curves of chillers, and attributes of the TES units. The analysis revealed that the proposed load regulation strategy has the potential to achieve energy savings ranging from 5.7% to 10.8% for chiller plants with poor COPs under unfavorable PLRs, particularly in buildings with significant load variations.

Keywords

load regulation
thermal energy storage
chiller plants
building energy efficiency

Article History

Received: 25 February 2024
Revised: 27 March 2024
Accepted: 14 April 2024

1 Introduction

Buildings consume about 40% of the total electrical energy generated from conventional power stations or renewable energy systems, contributing over one-third of the total carbon dioxide emission worldwide (Hu et al. 2022; Lu et al. 2023). The major part of the electrical energy, about 30%–40% of the total, is used by heating, ventilation and air-conditioning (HVAC) systems (Kaspar et al. 2022; Wu et al. 2024). To achieve carbon neutrality, it becomes necessary to enhance the efficiency and flexibility of building energy systems (Garimella et al. 2022; Liu et al. 2023), which offers incentives for the fast development of techniques of thermal energy storage (TES), especially those using phase change materials (PCMs).

TES is primarily employed to shift the cooling or heating load of buildings. This involves transferring the cooling or heating load of HVAC systems from peak periods to off-peak periods in order to save energy costs under time-of-use tariffs (Cox et al. 2019; Campos et al. 2021; Kang et al. 2022). For example, the study in Powell et al. (2013) shows that a simple load shifting method can save 17.4% cost compared with the system without any load shifting. To realize the load shifting, the charging or discharging of TES is always schedule-based, usually fully charged during the off-peak demand period (e.g., at night) and fully discharged during the on-peak demand period (e.g., at daytime). Load shifting, however, will increase the total energy consumption of HVAC systems because of the heating or cooling loss due to a long time storage (Sehar et al. 2012). TES has also gained applications in natural energy harvest for buildings, such as in free colling (Chiu et al. 2013; Alizadeh and Sadrameli 2016) or Trombe walls (Xiong et al. 2022), which reduces the cooling or heating load through natural energy

E-mail: gongsheng.huang@cityu.edu.hk

List of symbols

c	specific heat (kJ/kg)
E	energy (kWh)
$\dot{m}$	flowrate (kg/s)
P	power (kW)
Q	cooling load (kW)
R	ratio (%)
S	COP improving potential (%)
T	temperature (°C)
α, β	model coefficient (—)
γ	fraction coefficient (—)
δ	regulated load (kW)
θ	TES power coefficient (—)
λ	TES capacity coefficient (hour)
τ	time (hour)

Subscripts

ahuf	fan in air handling unit
bld	building
ch	chiller
chg	charging
chp	primary chilled water pump
chs	secondary chilled water pump
chws	chilled water supply temperature
ct	cooling tower
ctf	cooling tower fan
ctp	condenser water pump
cws	condenser water return temperature
dcg	discharging
sa	supply air
sub	sub-system
sys	system
wb	wet bulb temperature

Superscripts

max	maximum
min	minimum
opt	optimization
rt	rated condition

supplement. For example, a night ventilation with PCM packed bed storage system was developed in Kang et al. (2003) to make use of the temperature difference between daytime and nighttime and thus to minimize the electricity use of the HVAC systems. In TES-based natural energy harvest, the TES units should better be fully charged or discharged to maximize the use of the natural energy. Although TES-based natural energy harvest can reduce the energy use of buildings, it is not directly implemented to improve the energy efficiency of HVAC systems during their operation.

To fully explore the flexibility introduced by TES, TES should be actively involved in the operation of HVAC systems. This study, therefore, proposes a generic TES-based load regulation strategy for chiller plants to enhance the energy efficiency of chiller plants during their operation. The proposed strategy is motived by the observation that the coefficient of performance (COP) of a chiller plant is generally not a constant, varying inside a range, very wide sometimes. For example, the highest COP of a chiller could be over 7.0; while the lowest could be as low as 3.5 (ASHRAE 2011). Chillers are the key unit in a central air-conditioning system, accounting for 60% of the total energy consumed by the air-conditioning system. Therefore, to increase energy efficiency, chiller plants should be maintained to operate with high COPs, certainly as high as possible.

Many factors affect the COP of chiller plants (Hydeman and Gillespie 2002). One of the most important factors is part load ratio (PLR), which is the percentage of the chiller instantaneous cooling load to its rated cooling capacity. The relationship between the COP and PLR is characterized by a COP/PLR curve (Sun et al. 2009; Huang et al. 2016; Zhang et al. 2020). Different chillers may have a different COP/PLR curve, determined by the compressor types, such as screw roll, centrifugal, reciprocating or scroll, and operating settings, such as evaporating and condensing temperature (ASHRAE 2011). Due to the variation of the COP, the COP/PLR curves are not flat and have the highest value around a certain PLR.

Conventional chiller plants may only operate with high COPs inside a narrow favorable PLR range but poor COPs within wide non-favorable PLR ranges. Chiller plants are always sized according to the peak load of a building and the actual load of the building varies seasonally and daily due to the changes of external weather conditions and internal heat gains. Although a chiller plant could be configured with multiple chillers with different rated capacity to cope with part load operation with low COP (Huang et al. 2018), it cannot solve the problem fundamentally as the load can vary continuously but the combinations of operating chillers are limited, making it difficult to ensure all the chillers operating within the favorable PLR range. An analysis of the cooling energy consumption for an office building showed that when the cooling unit operation was not well

planned, 70% of its annual energy consumption was inside the low PLR range (0%–50%), leading to very low COPs in operation (Seo and Lee 2016). Therefore, load regulation for chiller plants during their operation becomes necessary to improve their energy efficiency.

Different from TES-based load shifting aiming at cost saving or TES-based natural energy harvest aiming at building load shaving, the proposed generic TES-based load regulation strategy aims to actively regulate the load of chiller plants so as to ensure chiller plants operating within a favorable PLR range, and thus minimizing the energy consumption of chiller plants without affecting the load demand from buildings for thermal comfort. Timely charging or discharging of the TES units with right amount of charging or discharging power is very necessary to maintain a chiller plant operating with high COPs. Therefore, partially charging or discharging of the TES units will be adopted in the load regulation strategy, unlike fully charging or discharging of the TES units in load shifting or natural energy harvest. The TES-based load regulation strategy will be formatted as a constrained nonlinear optimization problem, which will be solved to generate the charging or discharging power series during the regulation period according to the predicted building load profile. Comprehensive numerical studies were used to analyze the energy performance of the strategy by considering the variant properties of TES, typical COP/PLR curves and typical building load profiles.

The main contribution of this study is to provide a generic load regulation strategy to advance energy efficiency of chiller plants through actively involving TES into their normal operation, in which the charging and discharging power of the associated TES units are optimized to manipulate the chiller plants working in a narrow favorable PLR range with high COPs. The rest of the paper is organized as follows. The principle of the active load regulation technique is illustrated in Section 2. Section 3 presents a comprehensive numerical analysis on the energy performance of the load regulation technique. Potential application and relative discussions are presented in Section 4. At last, concluding remarks are given in Section 5.

2 Principle of the TES-based load regulation

2.1 Necessity of load regulation

A central chiller plant mainly consisting of chillers, cooling towers, and their associated pumps and fans, and their connections are shown in Figure 1(a). The power consumption of the chiller plant P_{sys} is contributed from the pumps in the primary chilled water P_{chp} and the secondary loop P_{chs}, the compressors of the chillers P_{ch}, the pumps in the condenser water loop P_{ctp}, and the fans in the cooling tower P_{ctf}, which can be formulated as (Hou et al. 2020):

$$P_{sys} = P_{chs} + P_{chp} + P_{ch} + P_{ctp} + P_{ctf} \quad (1)$$

Referring to Hou et al. (2020), the power consumptions of the chiller plant are the functions of the chilled

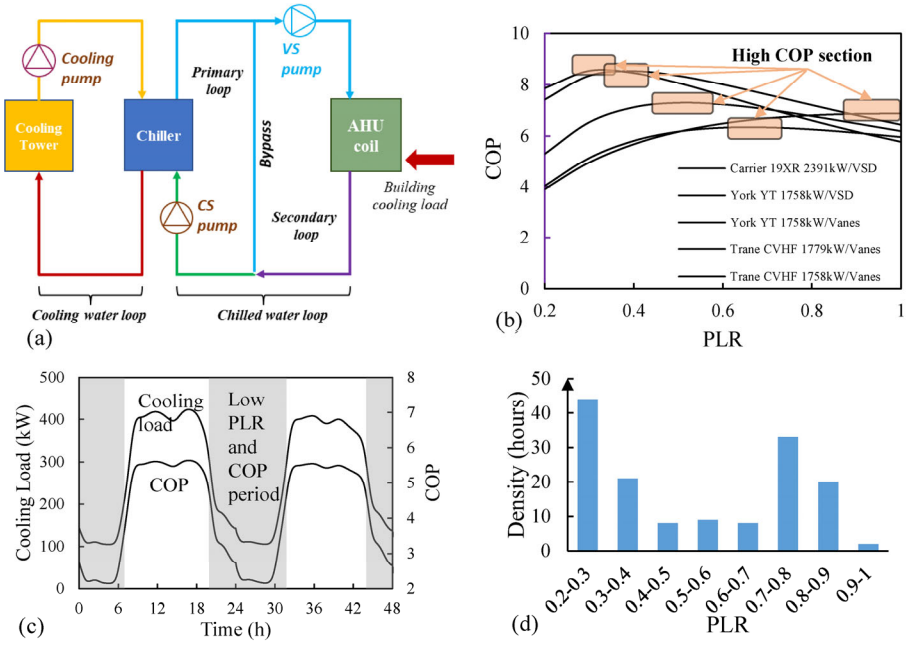

Fig. 1 (a) The schematic diagram of a central chiller plant, where its main components are shown inside the dot box; (b) typical COP/PLR curves for five different chillers using the dataset in EnergyPlus (Crawley et al. 2001); (c) the cooling load and corresponding COP of a chiller (Hou et al. 2020); (d) the chiller's PLR distribution of a commercial building in Hong Kong in a summer week (Hou et al. 2020).

water supply temperature T_{chws}, the condenser water return temperature T_{cws}, the building cooling load Q_{bld}, and the outdoor air wet bulb temperature T_{wb}. Thus Equation (1) can be rewritten as

$$P_{sys} = P_{chs}(Q_{bld}, T_{sa}) + P_{ch}(Q_{ch}, T_{chws}, T_{cws}) + P_{ctf}(Q_{ct}, T_{cws}, T_{wb}) + P_{chp} + P_{ctp} \quad (2)$$

where Q_{ch} and Q_{ct} are the cooling supply by the chiller and the heating rejected by the cooling tower, respectively. Generally, Q_{ch} is nearly the same with Q_{bld}. In practice, the chilled water supply temperature T_{chws}, the condenser water return temperature T_{cws} and the supply air temperature (T_{sa}) are generally maintained at constants (China Academy of Building Research 2021), such as T_{sa} = 15 °C, T_{chws} = 7 °C, T_{cws} = 30 °C. Therefore, the optimization of T_{chws}, T_{cws}, T_{sa} is not considered in this study in order to focus on the load regulation strategy. In this case, Equation (2) is simplified as

$$P_{sys} = P_{chs}(Q_{bld}) + P_{ch}(Q_{ch}) + P_{ctf}(Q_{ct}, T_{wb}) + P_{chp} + P_{ctp} \quad (3)$$

In an HVAC system, the chiller consumes almost two of thirds of the total energy. The energy performance of the chiller is characterized by its COP, defined by Equation (4), which, as well known, is strongly relative to its partial load ratio (PLR), defined by Equation (5).

$$\mathrm{COP}_{ch} = \frac{Q_{ch}}{P_{ch}} \quad (4)$$

$$\mathrm{PLR} = \frac{Q_{ch}}{Q_{ch}^{rt}} \quad (5)$$

where Q_{ch}^{rt} is the chiller rated cooling capacity. The relationship between the COP and PLR of a chiller is characterized by its COP/PLR curve. Different types of chillers may have different COP/PLR curves. Figure 1(b) shows five COP/PLR from five different chillers obtained when they are operating with their rated chilled water supply temperature and the rated cooling water return temperature (Crawley et al. 2001). It shows that except for TRANE 1758 kW/Vanes, the high COPs of others do not occur at their rated cooling capacity but at partial load conditions (Chang et al. 2005).

Meanwhile, the cooling load of a building is always time-varying due to the variation of climates, occupant density, lighting and equipment, resulting in time-variance in the load of its chill plant. Figure 1(c) presents the cooling load profile of a chiller plant for two successive days (Hou et al. 2020). It can be seen that this cooling load varies inside a wide range: the highest is over 400 kW; while the lowest is below 100 kW. As a consequence, the COP experiences a wide change as well: the highest is around 5.5; while the lowest is only 2.5. Figure 1(d) presents the PLR distribution using the measured cooling loads of a commercial building in Hong Kong within a summer week (Hou et al. 2020). It shows that this chiller plant works with a very low PLR during this period, resulting in a very low COP, being around 2.1.

Therefore, there is a high demand to improve the energy efficiency of chiller plants by intentionally regulating the cooling load to maintain a high COP during their operation. We thus propose a supply-side load regulation strategy, aiming to maintain chiller plants working with a high COP.

2.2 Principle of the TES-based load regulation

Assume the load regulation will be carried out during a period T (e.g. 24 hours), defined as the load regulation period, and the building cooling load inside T is sampled using a time instant Δt (e.g. 1 hour) as $Q_{bld,1}$, ..., $Q_{bld,n}$, or as $\vec{\boldsymbol{Q}}_{bld}$ in a compact form. The energy use of the system during the load regulation period E_{sys} (kWh) is given by

$$E_{sys} = E_{sub1} + E_{sub2} \quad (6)$$

where E_{sub1} is the energy consumption of the sub-system 1 including chiller and cooling tower, which are related to the cooling supply Q_{ch} of the chiller, the heat rejection Q_{ct} of the cooling tower and the wet bulb temperature T_{wb} of the outdoor air; E_{sub2} is the energy consumption of sub-system 2 including AHU, chilled water pump and cooling water pump, which are kept constant or only related to the building cooling load $Q_{bld,i}$. E_{sub1} and E_{sub2} can be written as

$$E_{sub1} = \Delta t \sum_{i=1}^{n} \left(P_{ch,i}(Q_{ch,i}) + P_{ctf,i}(Q_{ct,i}, T_{wb,i}) \right) \quad (7a)$$

$$E_{sub2} = \Delta t \sum_{i=1}^{n} \left(P_{chs,i}(Q_{bld,i}) + P_{chp} + P_{ctp} \right) \quad (7b)$$

It can be seen that the value of E_{sub2} is determined by the building cooling load profile. Therefore, E_{sub2} can be treated as a constant once the regulation period is specified. According to the definition of COP, the instantaneous power of a chiller at the i^{th} sampling time satisfies

$$P_{ch,i} = Q_{ch,i} / \mathrm{COP}_{ch,i} \quad (8)$$

The COP of a chiller can be approximated as a function of its PLR when the chiller works at the rated chilled water supply temperature and the rated cooling water return temperature (ASHRAE 2011), given by

$$\mathrm{COP}_{\mathrm{ch},i} = \mathrm{COP}_{\mathrm{ch}}^{\mathrm{rt}} \frac{\mathrm{PLR}_i}{\left(\alpha_0 \mathrm{PLR}_i^2 + \alpha_1 \mathrm{PLR}_i + \alpha_2\right)} \tag{9}$$

where α_0, α_1, α_2 are the coefficients, which could be identified through a curve fitting method. Substituting Equation (9) into Equation (8), the chiller power can be expressed as

$$P_{\mathrm{ch},i} = \frac{Q_{\mathrm{ch}}^{\mathrm{rt}}}{\mathrm{COP}_{\mathrm{ch}}^{\mathrm{rt}}}\left(\alpha_0\left(\frac{Q_{\mathrm{ch},i}}{Q_{\mathrm{ch}}^{\mathrm{rt}}}\right)^2 + \alpha_1\left(\frac{Q_{\mathrm{ch},i}}{Q_{\mathrm{ch}}^{\mathrm{rt}}}\right) + \alpha_2\right) \tag{10}$$

According to the work in Ma et al. (2008), the power of the cooling tower can be predicted by

$$P_{\mathrm{ctf}} = \beta_0 + \beta_1 \dot{m}_{\mathrm{ct,a}} + \beta_2 \left(\dot{m}_{\mathrm{ct,a}}\right)^2 \tag{11a}$$

$$\dot{m}_{\mathrm{ct,a}} = \beta_3 \left(Q_{\mathrm{ct}}\right)^{\beta_4} \left(T_{\mathrm{cws}} + \frac{Q_{\mathrm{ct}}}{c_{\mathrm{w}} \dot{m}_{\mathrm{cw}}} - T_{\mathrm{wb}}\right)^{\beta_5} \tag{11b}$$

where β_0, β_1, β_3, β_4, and β_5 are the model parameters of the cooling tower, which could be identified from historical data; $\dot{m}_{\mathrm{ct,a}}$ and $\dot{m}_{\mathrm{cw}}$ are the mass flow rate of the air flowing and water flowing of the cooling tower, respectively; c_{w} is the specific heat of the water.

In a chiller plant without load regulation, the cooling generated by the chiller plant is determined by the cooling load of the building. Ignoring the cooling loss of pipes and the heating gain of water pumps, the chiller cooling load should be equivalent to the building cooling load, i.e., $Q_{\mathrm{ch},i} = Q_{\mathrm{bld},i}$. Therefore, without load regulation, the power consumption of sub-system 1, E_{sub1} can be estimated by

$$E_{\mathrm{sub1}} = f_{\mathrm{ch}}\left(Q_{\mathrm{bld},i}\right) + f_{\mathrm{ct}}\left(Q_{\mathrm{bld},i} + P_{\mathrm{ch},i}, T_{\mathrm{wb},i}\right) \tag{12}$$

where f_{ch} and f_{ct} are the energy models of the chiller and cooling tower, respectively.

To regulate the load of a chiller plant without affecting the demand from buildings, TES units should be integrated into chiller plants. There are different ways to integrate TES into a chiller plant (Woods et al. 2021; Alam et al. 2022). Here, an integration that will not affect the cooling supply side is chosen, which is shown in Figure 2(a). In this integration, the chilled water with rated supply temperature could be used to charge the TES units without intentionally reducing its temperature, which has been demonstrated feasible in Woods et al. (2021) and Alam et al. (2022). The proposed load regulation strategy uses a TES unit to enlarge or reduce the chiller cooling load to minimize the energy use during a predefined regulation period. By the load regulation, the cooling load of the chiller at the i^{th} sampling

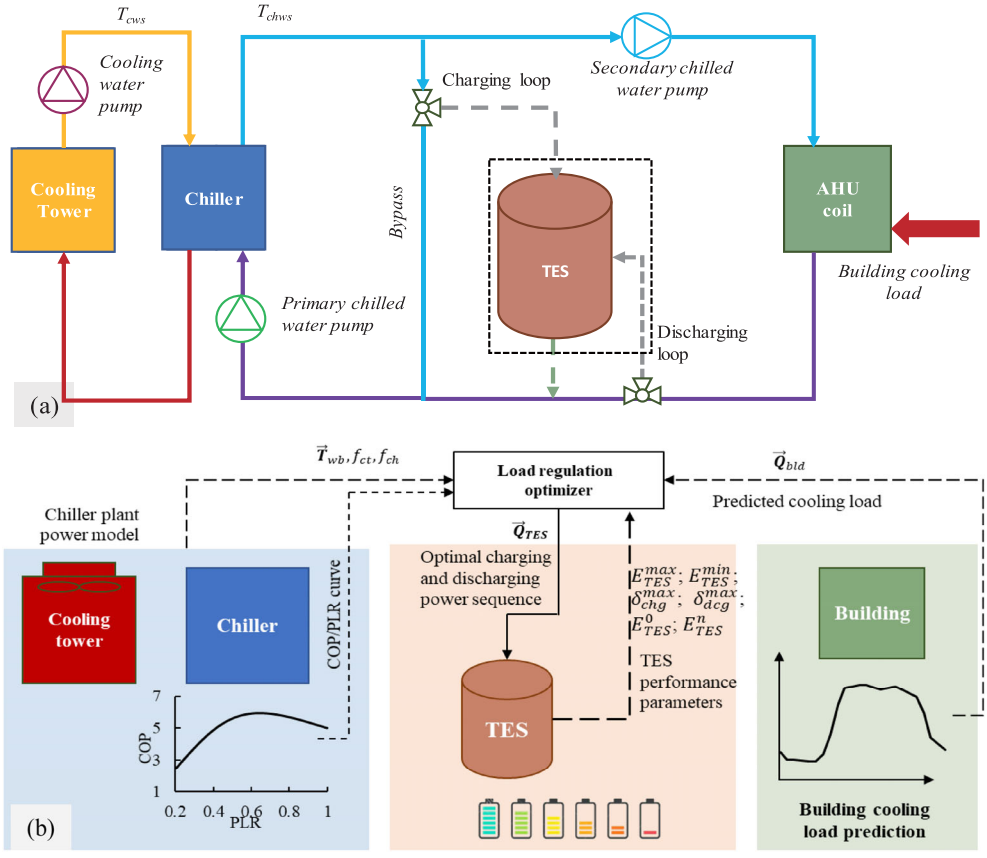

Fig. 2 (a) The integration of TES into a chiller plant; (b) schematic diagram of the proposed load regulation strategy framework for chiller plants

time is represented by

$$Q_{\mathrm{ch},i} = Q_{\mathrm{bld},i} + \delta_{\mathrm{LR},i} \tag{13}$$

where $\delta_{\mathrm{LR},i}$ is the cooling load that needs to be regulated at the i^{th} sampling time. When $\delta_{\mathrm{LR},i}$ is positive, the TES unit draws cooling energy from the chiller plant, enlarging the cooling load of the chiller; while when $\delta_{\mathrm{LR},i}$ is negative, the TES unit injects the cooling energy into the chiller plant, reducing its cooling load. After the load regulation, the power consumption of the chiller plant, $\tilde{E}_{\mathrm{sub1}}$, becomes

$$\tilde{E}_{\mathrm{sub1}} = f_{\mathrm{ch}}\left(Q_{\mathrm{bld},i} + \delta_{\mathrm{LR},i}\right) + f_{\mathrm{ct}}\left(Q_{\mathrm{bld},i} + \delta_{\mathrm{LR},i} + P_{\mathrm{ch},i}, T_{\mathrm{wb},i}\right) \tag{14}$$

The energy use of the chiller plants during the load regulation period T becomes

$$\tilde{E}_{\mathrm{sys}} = \tilde{E}_{\mathrm{sub1}}\left(\vec{\boldsymbol{Q}}_{\mathrm{bld}}, \vec{\boldsymbol{T}}_{\mathrm{wb}}, \vec{\boldsymbol{\delta}}_{\mathrm{LR}}\right) + E_{\mathrm{sub2}} \tag{15}$$

The objective of the regulation is to minimize the energy use during the regulation period, i.e.,

$$\left(\delta^{\mathrm{opt}}_{\mathrm{LR},1}, \delta^{\mathrm{opt}}_{\mathrm{LR},2}, \ldots, \delta^{\mathrm{opt}}_{\mathrm{LR},n}\right) = \min_{\delta_{\mathrm{LR},1}, \delta_{\mathrm{LR},2}, \ldots, \delta_{\mathrm{LR},n}} \tilde{E}_{\mathrm{sys}} = \min_{\delta_{\mathrm{LR},1}, \delta_{\mathrm{LR},2}, \ldots, \delta_{\mathrm{LR},n}} \tilde{E}_{\mathrm{sub1}} \tag{16}$$

where $\vec{\boldsymbol{\delta}}^{\mathrm{opt}}_{\mathrm{LR}}$ (or $\delta^{\mathrm{opt}}_{\mathrm{LR},1}, \delta^{\mathrm{opt}}_{\mathrm{LR},2}, \ldots, \delta^{\mathrm{opt}}_{\mathrm{LR},n}$) is the regulation power series, kW.

In practice, the load regulation should be subject to the operation constraints (OCs) for both the chillers and the TES unit, listed below:

- OC1: $\gamma Q^{\mathrm{rt}}_{\mathrm{ch}} \le Q_{\mathrm{bld},i} + \delta_{\mathrm{LR},i} \le Q^{\mathrm{rt}}_{\mathrm{ch}}$
- OC2: $E^{\min}_{\mathrm{LR}} \le E_{\mathrm{TES},0} + \Delta t \sum_{k=1}^{i} \delta_{\mathrm{LR},k} \le E^{\max}_{\mathrm{LR}}$
- OC3: $-\delta^{\max}_{\mathrm{dcg}} \le \delta_{\mathrm{LR},i} \le \delta^{\max}_{\mathrm{chg}}$
- OC4: $\sum_{i=1}^{n} \delta_{\mathrm{LR},i} = 0$

OC1 specifies the feasible operation range of a chiller according to its rated capacity $Q^{\mathrm{rt}}_{\mathrm{ch}}$. $\gamma Q^{\mathrm{rt}}_{\mathrm{ch}}$ is the lowest allowable capacity for normal operation without surge. OC2 specifies the feasible range for the cooling energy stored by the TES unit, specified as ($E^{\min}_{\mathrm{LR}}$, $E^{\max}_{\mathrm{LR}}$). In this study, the heat loss of the TES is ignored for simplification, as the heat loss of a well-insulated TES is little compared with the total cooling load of the chiller (Zou et al. 2023). OC3 is considered because the charging and discharging power of the TES unit should be limited in its feasible range, specified as ($-\delta^{\max}_{\mathrm{dcg}}$, $\delta^{\max}_{\mathrm{chg}}$), where $\delta^{\max}_{\mathrm{chg}}$ is the maximum allowable charging power and $\delta^{\max}_{\mathrm{dcg}}$ is the maximum allowable discharging power. For control and operation convenience, the total cooling absorbed by the TES unit should be the same as the total released during the regulation period, which leads to OC4. Considering the above operation constraints, the optimization defined in Equation (16) becomes

$$\left(\delta^{\mathrm{opt}}_{\mathrm{LR},1}, \delta^{\mathrm{opt}}_{\mathrm{LR},2}, \ldots, \delta^{\mathrm{opt}}_{\mathrm{LR},n}\right) = \min_{\delta_{\mathrm{LR},1}, \delta_{\mathrm{LR},2}, \ldots, \delta_{\mathrm{LR},n}} \tilde{E}_{\mathrm{sub1}}, \quad \text{subject the OC1–OC4} \tag{17}$$

Thus, the TES-based load regulation is a constrained nonlinear optimization problem. Figure 2(b) shows the schematic diagram of the load regulation strategy, where the main components of the regulation strategy include: the COP/PLR curves of the chillers, the performance parameters of the TES units, the power models of the chiller plant, and the predicted building load profile in the regulation period.

To implement this strategy, the COP/PLR curve coefficients α_0, α_1 and α_2, the chiller rated cooling capacity $Q^{\mathrm{rt}}_{\mathrm{ch}}$ and its minimum allowable cooling capacity $\gamma Q^{\mathrm{rt}}_{\mathrm{ch}}$, the coefficients β_0 to β_5 of the cooling tower power model should be identified based on the measured or the manufacturer-provided data (Liu et al. 2017). Usually, γ should be set as 0.15 for most of chillers to avoid surging. The constraints for the TES unit, $E^{\max}_{\mathrm{LR}}$, $E^{\min}_{\mathrm{LR}}$, $\delta^{\max}_{\mathrm{chg}}$, $\delta^{\max}_{\mathrm{dcg}}$ and $E_{\mathrm{LR},0}$ should be specified to ensure the load being regulated properly. Normally, $E^{\max}_{\mathrm{LR}}$ and $E^{\min}_{\mathrm{LR}}$ could be set as 90% and 10% state of charge (SOC) of the TES unit as in this range the heat exchanging rate could be stable and easy to control (Arena et al. 2018; Woods et al. 2021). The cooling load profile $\vec{\boldsymbol{Q}}_{\mathrm{bld}}$ of the building and the wet bulb temperature of the outdoor air $\vec{\boldsymbol{T}}_{\mathrm{wb}}$ during the regulation period should be predicted according to building physics, weather conditions, internal heat gains or historical load data. Usually, the regulation period T should be set to 24 hours for a reliable predicted cooling load profile (Candanedo et al. 2013; Kang et al. 2022).

With these parameters and inputs, the load regulation strategy will output the optimized regulation sequence of $\delta^{\mathrm{opt}}_{\mathrm{LR},1}, \delta^{\mathrm{opt}}_{\mathrm{LR},2}, \ldots, \delta^{\mathrm{opt}}_{\mathrm{LR},n}$. The dynamic programming solver in MATLAB, *DynaProg* toolbox developed by Miretti et al. (2021), for example, can be used for solving the optimization problem. The regulation interval is suggested to be one hour, which is long enough to tolerate the dynamics of the TES charging/discharging. The optimized regulation amounts $\delta^{\mathrm{opt}}_{\mathrm{LR},1}, \delta^{\mathrm{opt}}_{\mathrm{LR},2}, \ldots, \delta^{\mathrm{opt}}_{\mathrm{LR},n}$ are then sequentially executed through a charging and discharging control, for example model predictive control (MPC) (Candanedo et al. 2013; Yang et al. 2022) based on the TES model (Wan et al. 2022).

3 Regulation performance analysis

To analyze the regulation performance, a typical HVAC system was considered in the case studies. The system consists of one chiller, one primary chilled water pump, one secondary chilled water pump, one condenser water pump, one cooling tower, one air handling unit, and one TES tank. The chiller has a rated capacity of 509 kW and a rated COP of 6.5. The COP/PLR curve of the chiller is identical to that of Trane CVHF Vanes. The maximum COP of the chiller is 7.67, which is achieved at a PLR of 0.51. The cooling tower has a rated capacity of 604 kW and a rated power of 5.5 kW. The regulation period was set as 24 hours, from 0:00 to 24:00. The TES parameters were set as: $E_{\mathrm{TES}}^{\max} = 1.8 \times 509$ kWh; $E_{\mathrm{TES}}^{\min} = 0.2 \times 509$ kWh; $E_{\mathrm{TES},0} = 1 \times 509$ kWh; $\delta_{\mathrm{chg}}^{\max} = \delta_{\mathrm{dcg}}^{\max} = 0.25 \times 509$ kW. Figure 3(a) compared the load profile before and after regulation. It can be seen that the cooling load was regulated to three stages: the TES discharging stage (00:00–7:00 and 21:00–24:00), unchanged stage (7:00–9:00 and 20:00–21:00) and the TES discharging stage (9:00–20:00).

During the TES discharging stage, the cooling load of the chiller was raised to 175 kW from 00:00 to 7:00 and to 270 kW from 21:00 to 24:00. This corresponds to a chiller PLR of 0.34 and 0.53, as illustrated in Figure 3(b). Due to the load regulation, the chiller COP was increased from 5.8 to 7.2 during 00:00–7:00 and from 7.2 to 7.7 during 21:00–24:00, as shown in Figure 3(c). The TES was charged during these time periods, as depicted in Figure 3(g). This led to an increase in the SOC of the TES from 50% to 90% and from 10% to 50% respectively, as shown in Figure 3(f). During the TES discharging stage, the cooling load of the chiller was reduced from 400 kW to 334 kW during 9:00–20:00, as shown in Figure 3(a), corresponding to the PLR of 0.66, as shown in Figure 3(b). Due to this load regulation, the chiller COP was increased from 7.1 to 7.5, as shown in Figure 3(c). The TES power was discharged during this period, and the TES was discharged from 90% (i.e., $E_{\mathrm{TES}}^{\max}$) to 10% (i.e., $E_{\mathrm{TES}}^{\min}$). During the load unchanged stage, the chiller operated within a favorable PLR range of 0.4 to 0.7, as depicted in Figure 3(b). This corresponded to a relatively high COP of 7.5, as shown in Figure 3(c). Consequently, the TES system remained neither charged nor discharged, resulting in the SOC of the TES being maintained at 90% ($E_{\mathrm{TES}}^{\max}$) from 7:00 to 9:00 and at 10% ($E_{\mathrm{TES}}^{\min}$) from 20:00 to 21:00.

The accumulated building load during the regulation period was 6,822.6 kWh, which was not changed by the regulation. The regulated accumulated load was 813.8 kWh, being 11.9% of the accumulated building load, which indicated an insignificant demand for the storage capacity. The power curves of the chiller and the cooling tower are shown in Figures 3(d) and 3(e), respectively. With the load regulation, the energy consumption of the chiller was reduced from 973.3 kWh to 912.6 kWh, resulting in a 6.2% energy saving. The energy consumption of the cooling tower was slightly enlarged from 86.6 kWh to 87.1 kWh. The power curves of the chiller plant (i.e., the total power of the chiller and cooling tower) before and after the load regulation are shown in Figure 3(f). The energy consumption of the chiller plant was 1,059.9 kWh without the regulation, but it was reduced to 999.7 kWh after regulation, saving by 5.7%.

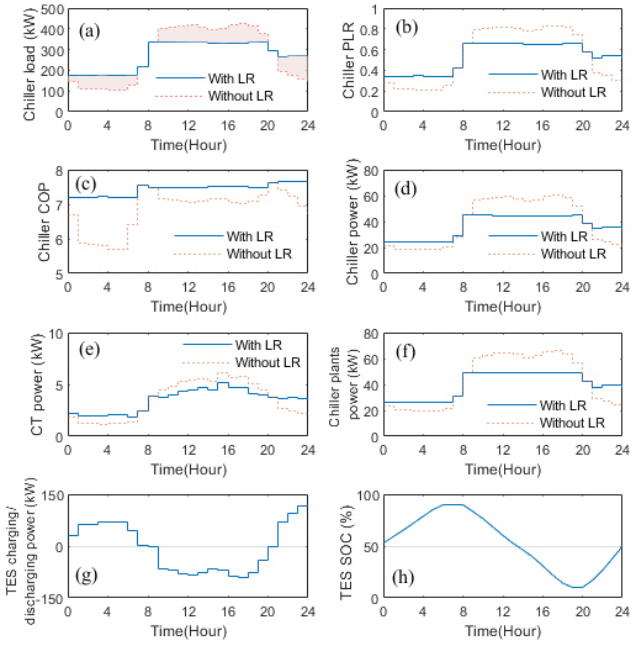

Fig. 3 The performance of the load regulation, where the abbreviation "LR" means load regulation. (a) Comparison of the chiller cooling load before and after the load regulation; (b) comparison of the chiller PLR before and after the load regulation; (c) comparison of the chiller COP before and after the load regulation; (d) comparison of the chiller power before and after the load regulation; (e) comparison of the cooling power before and after the load regulation; (f) comparison of the chiller plant power before and after the load regulation; (g) charging and discharging power in the load regulation; (h) TES soc variation within the load regulation

4 Advancements in energy performance from TES-based load regulation

4.1 Typical COP/PLR curves and cooling load profiles

To comprehensively analyze the advancements of the proposed load regulation strategy, typical chiller COP/PLR curves and typical cooling load profiles of several types of building were considered in the examination. Figure 4(a) presents the COP/PLR curves, where the relative COP is

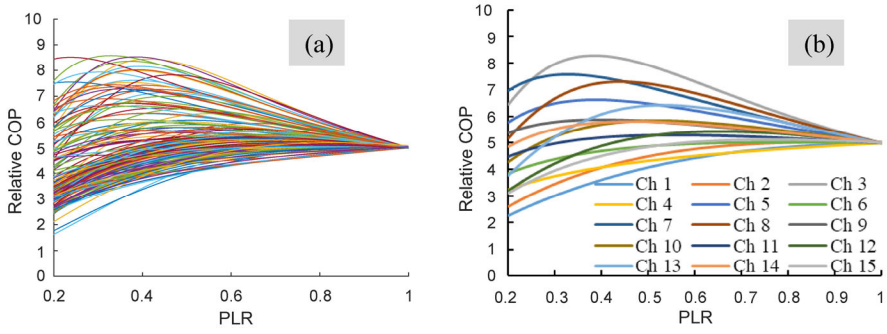

Fig. 4 COP/PLR curves of different chillers: (a) 160 COP/PLR curves summarized by Open Source Modelica Consortium and (b) 15 clustered COP/PLR curves by *k*-means clustering algorithm (Li et al. 2021)

defined as the COP in Equation (4) normalized by the COP at the chiller rated cooling capacity. These curves are from 160 different chillers in the mainstream market, summarized by Open Source Modelica Consortium (OpenModelica n.d.). To streamline the analyses, these COP/PLR curves were clustered using a *k*-means clustering algorithm (Li et al. 2021). The *k*-means clustering algorithm was developed to partition n samples into k clusters, in which each sample belongs to a cluster with the nearest mean. Then, the massive original samples can be significantly reduced into k prototypes while maintaining the original samples' characteristics. In this study, the hyperparameter k in the *k*-means clustering algorithm and the number of clustered COP/PLR curves were determined using a gap statistic method (Tibshirani et al. 2001). Figure 4(b) illustrated the clustered COP/PLR curves, where total 15 clusters were identified. Different clusters represent different COP variation patterns. For example, the COPs of Ch1 and Ch4 achieve their maximum at the PLR of 1; the COPs of Ch5 and Ch8 exhibit an increase and then a decrease with the PLR increase, i.e., their peak COPs occur at a part load. For those curves with the peak COP values at part loads, the part load ratios are different. For example, Ch3 and Ch5 achieve their peak COPs at lower part load ratios; while Ch12 and Ch13 reach their peak COPs at higher part load ratios.

The cooling load profiles of four typical prototype buildings under four typical climate zones, given by U.S. DOE (Deru et al. 2011), were used for analysis. The four buildings include a hospital (HP), a large hotel (LH), a large office (LO) and a secondary school (SS). The climate zones include very hot and humid zone (1A), hot and dry zone (2B), warm and marine zone (3C) and mild and marine zone (4C), representing typical climates where cooling is required. The details of these buildings and climate zones can be found in Ref. (Huang et al. 2018).

With the properties of the four typical buildings and the weather profiles of typical meteorological year (TMY) of the four typical climate zones, their yearly cooling load can be simulated using a popular building energy simulation software EnergyPlus (Crawley et al. 2001). The yearly cooling load profiles were re-arranged in a daily-cycle style, as the TES-based load regulation strategies are usually performed daily. Figure 5 gives the cooling load profiles of these prototype buildings under different climate zones, marked as "building type" and "climate". For example, HP_1A represents the cooling load profiles of the hospital in Zone 1. It shows that these cooling load profiles are diversified. For instance, the cooling load profiles of a specific building in different climates are different. Compared with 3C climate, the temperature difference of daily and nightly in Zone 1A is smaller, resulting in a flatter daily cooling load profile. By comparing the load profiles of different buildings under the same climate, the variation trends are also different, due to the difference of the daily schedule. The cooling load of HP is high during the day and low at night while the cooling load of LH is inverse. Besides, the cooling load profiles of LH are more stable compared to that of HP. Note that the cooling load profiles were normalized to 0–1000 kW to make it easy to analyze. Correspondingly, the sizes of the chiller plants are also equally scaled.

4.2 The influence of TES attributes

The impact of two key attributes of TES units on the energy-saving potential of the regulation strategy was examined before the energy saving potential analysis. These attributes include the full storage capacity and the maximum charging/discharging power. The TES full storage capacity was set as $\lambda \times Q_{ch}^{rt}$, where λ is hours and Q_{ch}^{rt} is the chiller rated cooling capacity. For example, if λ is 2 and Q_{ch}^{rt} is 100 kW, the full storage capacity should be 200 kWh. The TES maximum charging/discharging power was set as $\theta \times Q_{ch}^{rt}$, where θ is the ratio of the TES maximum charging/discharging power to the chiller rated cooling power. For example, if θ is 1/4 and Q_{ch}^{rt} is 100 kW, the TES maximum charging/discharging should be 25 kW. In the

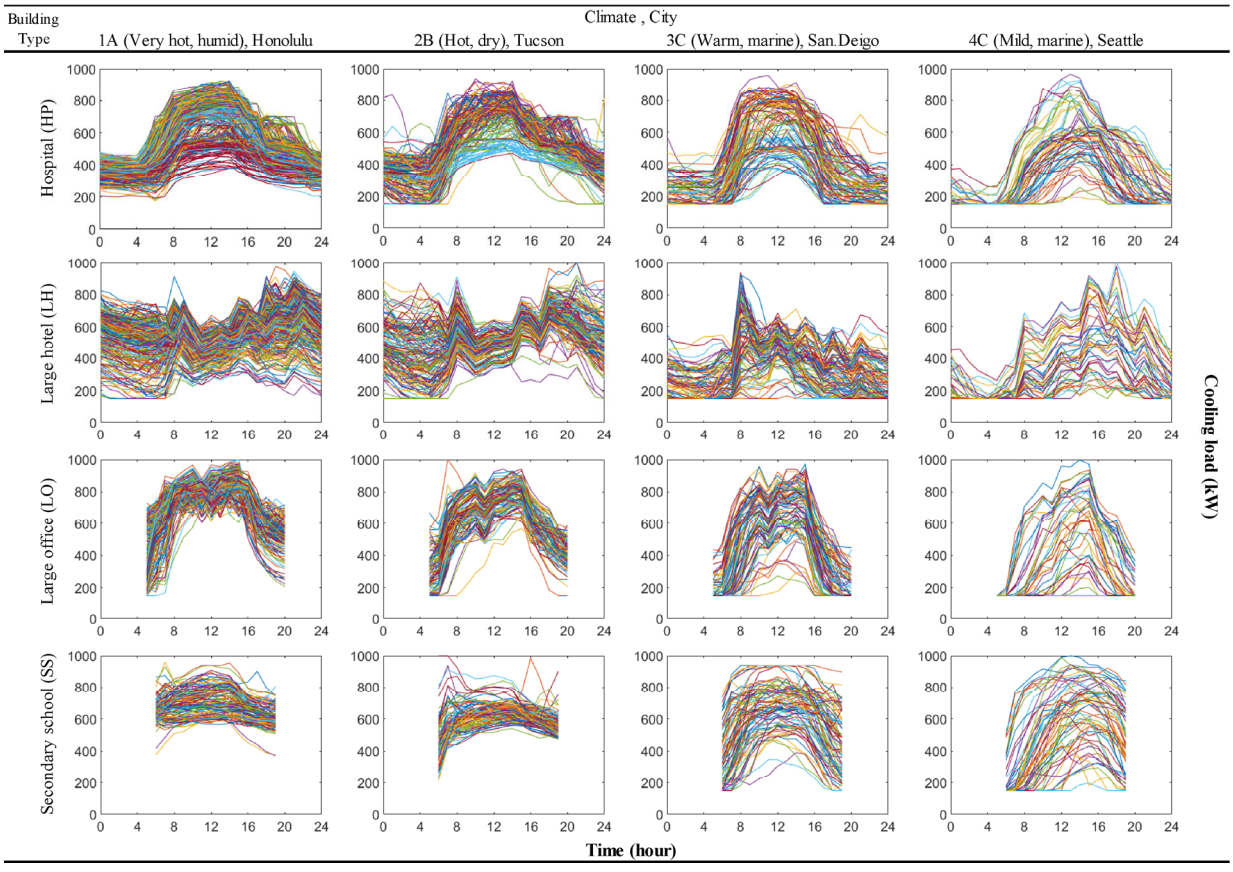

Fig. 5 Annual cooling load profiles of four prototype buildings under four climate zones. To illustrate the details of the load variations, the annul cooling load profiles were separated and presented as daily load profiles

following analysis, λ was chosen inside the range from 0.5 to 4; while θ was specified in the range from 1/6 to 1/3. Table 1 lists the values of λ and θ.

Considering the number of the clustered COP/PLR curves, shown in Figure 4(b), and the building types with four climate zones, shown in Figure 5, there are 6,720 (28 × 15 × 16) cases in total. The load regulation strategy was applied to all the cases, where the initial TES SOC was set to 50%. The results showed that with the increase of the TES storage capacity, the energy savings from the load regulation increased. The energy savings increased rapidly when the storage capacity was enlarged from 0.5 Q_{ch}^{rt} (kWh) to 1.5 Q_{ch}^{rt} (kWh), and then the increment became slow when the storage capacity was enlarged from 1.5 Q_{ch}^{rt} (kWh) to 3 Q_{ch}^{rt} (kWh). After 3 Q_{ch}^{rt} (kWh), the energy savings were saturated, suggesting that increasing the TES storage capacity would not yield any additional energy-saving potential. As an example, Figure 6 illustrates the influences of the annual energy savings resulting from different TES unit design parameters, in which four clustered COP/PLR curves (Ch1, Ch5, Ch12, and Ch13) and four cooling load profiles (HP_2B, LH_2B, LO_2B, and SS_2B) were chosen as examples. Therefore, the TES full storage capacity for the load regulation should be chosen not over 3 Q_{ch}^{rt} (kWh).

Table 1 Values of two key attributes of TES units used in the analysis

Parameter	Unit	Case
Full storage capacity	λQ_{ch}^{rt} (kWh)	λ = [0.5, 1, 1.5, 2, 2.5, 3, 4]
Maximum charging/ discharging power	θQ_{ch}^{rt} (kW)	θ = [1/6, 1/5, 1/4, 1/3]

The results presented in Figure 6 also show that increasing the TES maximum charging/ discharging power of the TES units can improve the yearly energy savings of the load regulation strategy. The increase of the TES maximum charging/discharging power of the TES resulted in the increase of the yearly energy savings. When the maximum charging/discharging power was higher than 1/4 Q_{ch}^{rt}, the energy savings were saturated, suggesting that increasing the TES maximum charging/ discharging power would contribute any additional energy-saving potential. This observation is similar to that observed in studying the TES full storage capacity. Hence, it is advisable to select the TES maximum charging or discharging power to be no more than 1/4 Q_{ch}^{rt} in the proposed regulation strategy.

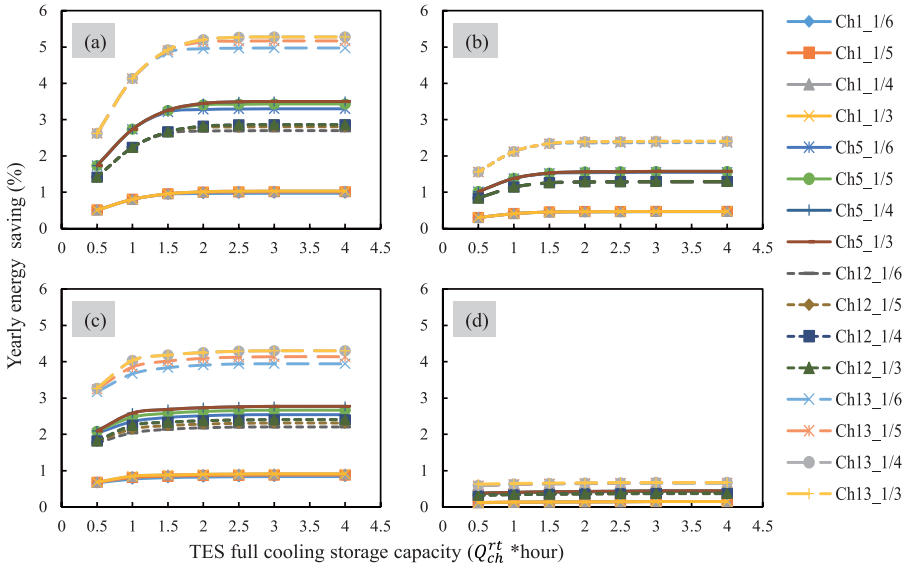

Fig. 6 The influence of TES storage capacity and charging/discharging power on the yearly energy savings of the load regulation strategy with typical COP/PLR curves: (a) hospital, (b) large hotel, (c) large office and (d) secondary school under climate Zone 2B. CH1_1/6 refers the 1st clustered COP/PLR curve with the maximum charging/discharging power of 1/6 Q_{ch}^{rate}

4.3 Energy saving potential analysis

Following the studies in Section 4.2, in the following analysis of the energy saving potential, the TES full storage capacity was set to be 3 Q_{ch}^{rt} (kWh) and the TES maximum charging or discharging power was set to be 1/4 Q_{ch}^{rt}. With these settings, the load regulation strategy was applied to all the combinations of these 15 clustered COP/PLR curves and these four building types with four climate zones. The annual energy savings were sorted in Figure 7, which shows that the COP/PLR curves, building types, and climate zones have significant impact on the load regulation performance. The maximum energy saving was as high as 12% achieved by the combinations of Ch3 with LO_3C (i.e., large office building under climate zone 3C), HP_3C and HP_4C. The minimum energy saving was slightly over 0.5%, achieved by the combination of Ch4 with SS_1A.

To identify which type of cooling load profiles being suitable for the use of the proposed load regulation strategy, the energy saving percentages were plotted with respect to the combinations of these four building types and four climate zones. Each combination has 15 energy saving percentages and each percentage is corresponding to an individual COP/PLR cluster. Figure 8(a) shows these percentages and their distributions using violin plots. Taking the combination of LO_3C as an example, the upper violin plot shows the energy savings distribution of the 15 clustered chillers. The energy savings varied from approximately 1% to 11%, three out of four exceeding 2.5% and one out of four surpassing 7.5%. The median saving, denoted by a white point in the plot, was around 4%,

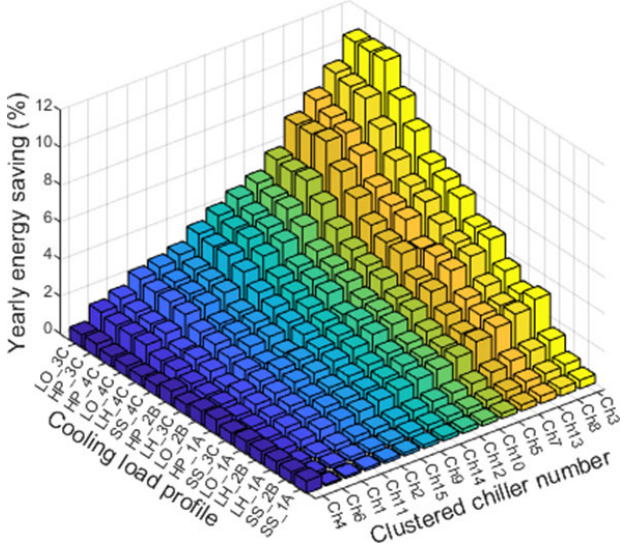

Fig. 7 Yearly energy saving percentages of the load regulation strategy when it was applied to the combinations of 15 clustered COP/PLR curves and 4 building types with 4 climate zones

indicating that half of the energy savings was over 4%. According to the median value of each combination, the combinations of building types and climates were divided into four groups: Group I (median saving < 1%), Group II (1% ≤ median saving < 2%), Group III (2% ≤ median saving < 3%) and Group IV (median saving ≥ 3%). Figure 8(b) depicts the distributions of the daily load variation amplitudes, which are defined as the disparity between the maximum and minimum cooling load values, divided by the rated capacity of the chiller. Figure 8(b) also adopts the violin plot. To explain in detail, the combination

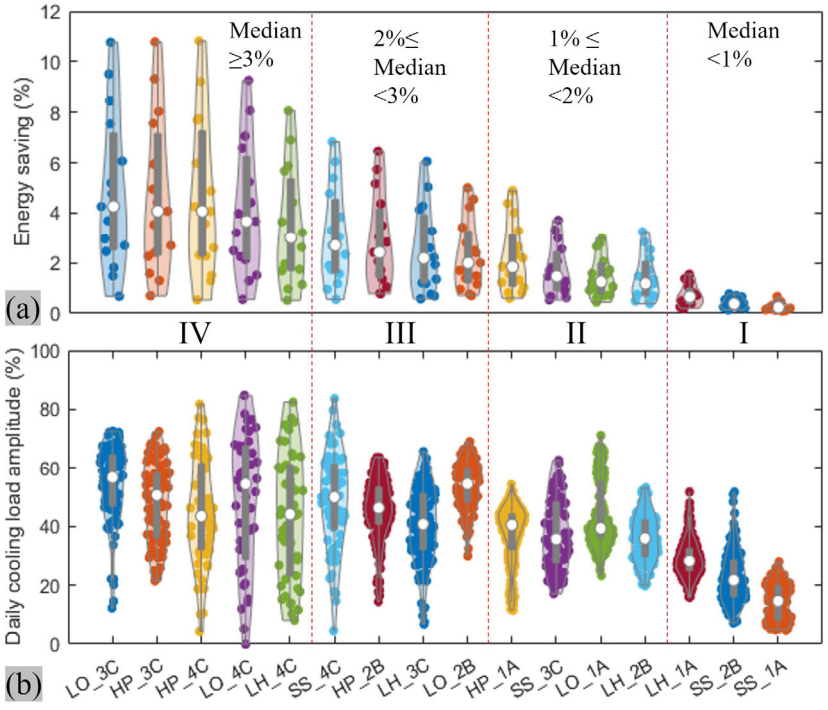

Fig. 8 (a) The distribution of yearly energy saving percentage of each combination of building types and climate zones, where the white dot is the median value of these energy saving percentages; (b) the distribution of the corresponding daily load variation amplitudes

of LO_3C was used as an example again. The load variation amplitudes of the 95 cooling days of LO_3C were within the range from 10% to 75%, with three-quarters exceeding 45% and one-quarter surpassing 65%. The majority of the load variation amplitudes fall between 45% and 75%, which is indicated by the probability density edge line (the gray line in the figure). Considering both energy savings and daily cooling load variation amplitude, it becomes evident that a higher daily building load variation amplitude benefits the performance of the load regulation strategy. This is because the COP of the chiller might vary significantly when the building load changed greatly, leaving the load regulation strategy much space to regulate the load profile. In Groups III and IV, most of the daily load variation amplitudes were higher than 40%, resulting in a high energy saving potential. On the contrary, there was little space for load regulation when the building load profiles was flat. For example, in Group I, most of the daily load variation amplitudes were below 30%, making energy saving potential insignificant.

To identify which clusters of the COP/PLR curves being suitable for the use of the proposed load regulation strategy, the energy savings were plotted with respect to the cluster number. For each cluster, there were 16 combinations from those 4 building types and 4 climate zones. Figure 9 displays the violin plots of the savings for each cluster, arranged in ascending order according to the mean value of the 16 savings. Based on their energy-saving percentages, the COP/PLR clusters were also divided into four groups: group A (median saving < 1%), group B (1% ≤ median saving < 2%), group C (2% ≤ median saving < 3%), and group D (median saving ≥ 3%). Figure 9(b) shows the corresponding COP/PLR curves in each group. Noted that the load regulation strategy demonstrated favorable performance for the COP/PLR curves in Group C and Group D, while it did not perform as well for Group A and Group B. This is because the COP/PLR curves in Group C and Group D have larger difference between their peak COP and minimum COP in their feasible range compared with the curves in Group A and Group B. Generally, a larger difference offers more space for load regulation and thus more enhancement in energy saving. Another observation is that to benefit the load regulation, the peak COP should better occur at a part load other than at the full load. This is because the load regulation strategy tends to reduce the chillers' load by charging the TES when the chiller load is high, while to increase the chiller's load by discharging the TES when the chiller load is low. If the peak COP occurs at a part load, both charging at low load conditions and discharging at high load conditions might directly result in COP increase. If the peak COP occurs at the full load condition, it is impossible to ensure the COP increase through both charging and discharging.

Note that the COP/PLR curves are primarily influenced by the compressor types, motor operation modes, and cooling capacities. Typically, variable-speed chillers are more

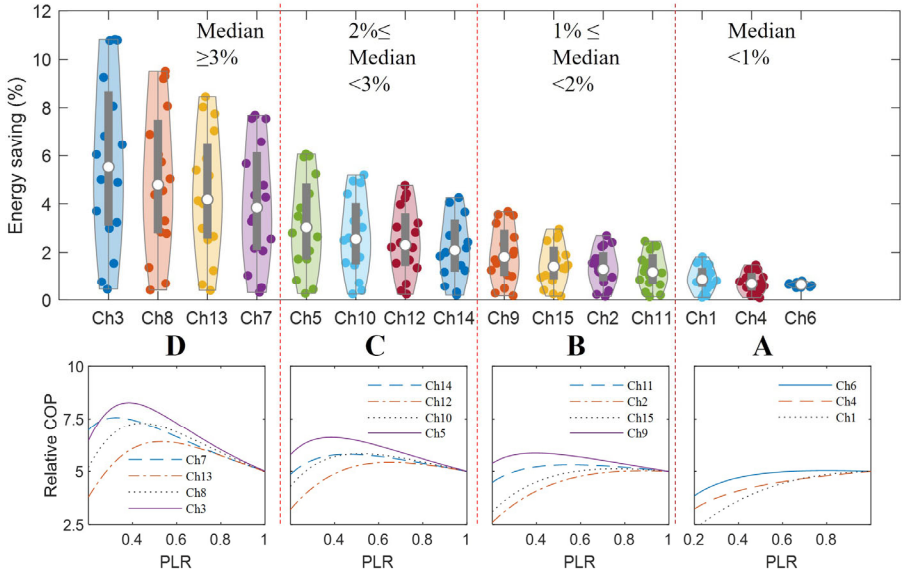

Fig. 9 (a) Yearly energy saving distribution of each cluster of the COP/PLR curves, which was divided into four groups: A, B, C, D; (b) the corresponding COP/PLR curves in each group

efficient at lower partial load ratios than constant-speed chillers due to their adopted different capacity control methods. For example, a constant-speed centrifugal chiller normally controls the cooling capacity by adjusting the openness of the guide vanes on the compressor inlet; while the compressor keeps running at the full speed, leading to the decrease of efficiency. In contrast, a variable-speed chiller controls its cooling capacity by adjusting the frequency of the motor, keeping the compressor operating more efficiently. Therefore, variable speed chillers are more likely to be classified under Group C and Group D. Conversely, constant speed chillers are more likely to fall under Group A and Group B and are not well-suited for implementing load regulation strategies.

Table 2 provides a summary of the energy-saving potential based on the groups of COP/PLR clusters and the groups of daily load variation amplitudes. It shows that the proposed strategy will have the highest energy-saving potential in the scenario that (1) a chiller plant has a COP/PLR curve similar to those in Group D, characterized by a significant difference between peak COP and minimum COP, with the maximum COP occurring at a part load; and (2) the daily cooling load variation amplitude is similar to those in Group IV, indicating a large daily variation in cooling load. In other scenarios, the energy-saving potential may be insignificant, particularly when the COP/PLR curve resembles those in Group A and the daily load variation amplitude is similar to those in Group I. Table 2 can serve as a guideline to evaluate the feasibility of implementing the load regulation strategy based on the given COP/PLR curve and daily load variation amplitude.

4.4 Discussions

The proposed load regulation strategy is a straightforward and practical approach. Firstly, it focuses solely on regulating the cooling load of chiller plants, without impacting the operation of cooling supply systems and the cooling load of buildings. This makes it easy to integrate the thermal energy storage (TES) units into existing chiller plant systems. Secondly, the load strategy allows the TES units to be charged by the primary chillers, eliminating the need for an additional dedicated chiller for charging. This minimizes retrofitting requirements. Despite its simplicity, the load

Table 2 Energy saving potentials of chiller groups and cooling load profiles

Yearly energy saving		Group of COP/PLR clusters			
		A	B	C	D
Group of daily	IV	0.5%–1.8%	1.7%–3.7%	3.0%–6.1%	5.7%–10.8%
cooling	III	0.6%–1.2%	1.2%–2.3%	2.0%–3.8%	3.4%–6.8%
cooling	II	0.4%–0.8%	0.7%–1.6%	1.2%–2.6%	2.1%–4.9%
cooling	I	0.1%–0.7%	0.1%–0.5%	0.2%–0.8%	0.3%–1.6%

regulation strategy holds potential for improving the energy efficiency of chiller plants.

To realize the proposed load regulation strategy, phase changing materials (PCMs) with suitable melting temperature could be a preferable thermal storage medium other than water due to their high power density (Zhang and Niu 2016). The suitable melting temperature is suggested to set as the average between the rated chilled water supply and return temperature. For example, the melting temperature could be chosen to be 8 °C, such as the S8 salt hydrate PCM from PCMproducts Ltd (PCM Products 2024), if the rated chilled water supply and return temperature are 5 °C and 12 °C respectively. Another important issue is the building load prediction for the load regulation. Until now, there are many methods available in literature or practices to predict the building cooling load (Campos et al. 2021; Kang et al. 2022; PCM Products 2024). These methods with high accuracy and reliability can be directly adopted in this regulation strategy to enhance the robustness of load regulation.

Note that the numerical analyses in this study have not consider the impact of the optimal control of the chilled water supply temperature and the cooling water return temperature in chiller plants. As a consequence, the findings of this study are constrained to the utilization of the chiller plants with fixed set-points for the chilled water supply temperature and the cooling water return temperature. In our future work, the proposed load regulation strategy will be extended for the chiller plants with optimal control of the chilled water supply temperature and the cooling water return temperature. Additionally, economic analyses will be conducted to evaluate the practical implications of this strategy.

5 Concluding remarks

This study presents a new strategy for advancing the building energy efficiency, a generic load regulation strategy for chiller plants, which aims to address the problem that many chiller plants may only operate with high COP under a very few favorable PLRs but low COP under many other non-favorable ones. Through timely charging or discharging the associated TES units with optimized charging or discharging power during the load regulation period, the proposed load regulation strategy is able to keep chiller plants working with high COPs, and thus reduce the energy use of the chiller plants without affecting the cooling demand from buildings. The main findings were summarized as below:

- The regulation strategy is fundamentally a constrained nonlinear optimization problem. Different from the load shift that normally charge or discharge the TES units based on a predefined schedule, the load regulation needs to control the charge and discharge power to maximize the energy saving.
- The performance of the load regulation strategy is significantly affected by the attributes of the TES units, including the TES full storage capacity and the TES maximum charging and discharging power. Trough comprehensive analyses, the TES full storage capacity and the TES maximum charging or discharging power are suggested to be three times and one quarter of the rated cooling capacity of the chiller plant, respectively.
- Numerical analyses were conducted to investigate the impact of building load profiles and the COP/PLR curves of chillers. The load regulation should have the best performance in energy saving when the building load has a large variation during its regulation period and the COP/PLR curve is characterized by a significant difference between peak COP and minimum COP, with the maximum COP occurring at a part load. When the COP/PLR curve is similar to those in Group D and the daily cooling load variation amplitude is similar to those in Group IV, the load regulation strategy may result in the energy saving from 5.7% to 10.8%.

Therefore, the proposed load regulation strategy is a promising measure to be applied to chiller plants for energy minimization during their operation.

Acknowledgements

The authors would like to acknowledge the funding support by a CRF from UGC Hong Kong (C5018-20G), a MFPRC from City University of Hong Kong (9680328), and a Guangzhou International Science and Technology Cooperation project (2021A0505030077).

Funding note: Open access publishing enabled by City University of Hong Kong Library's agreement with Springer Nature.

Declaration of competing interest

The authors have no competing interests to declare that are relevant to the content of this article. Shengwei Wang is an Editorial Board member of *Building Simulation*.

References

Alam M, Devapriya S, Sanjayan J (2022). Experimental investigation of the impact of design and control parameters of water-based active phase change materials system on thermal energy storage. *Energy and Buildings*, 268: 112226.

Alizadeh M, Sadrameli SM (2016). Development of free cooling based ventilation technology for buildings: thermal energy storage (TES) unit, performance enhancement techniques and design considerations—A review. *Renewable and Sustainable Energy Reviews*, 58: 619–645.

Arena S, Casti E, Gasia J, et al. (2018). Numerical analysis of a latent heat thermal energy storage system under partial load operating conditions. *Renewable Energy*, 128: 350–361.

ASHRAE (2011). ASHRAE Handbook—HVAC applications (SI). Atlanta, GA, USA: American Society of Heating, Refrigerating and Air-Conditioning Engineers.

Campos G, Liu Y, Schmidt D, et al. (2021). Optimal real-time dispatching of chillers and thermal storage tank in a university campus central plant. *Applied Energy*, 300: 117389.

Candanedo JA, Dehkordi VR, Stylianou M (2013). Model-based predictive control of an ice storage device in a building cooling system. *Applied Energy*, 111: 1032–1045.

Chang Y-C, Lin J-K, Chuang M-H (2005). Optimal chiller loading by genetic algorithm for reducing energy consumption. *Energy and Buildings*, 37: 147–155.

China Academy of Building Research (2021). White Paper on the Application Status Quo of Building Intelligence Based on Surveys. (in Chinese)

Chiu JNW, Gravoille P, Martin V (2013). Active free cooling optimization with thermal energy storage in Stockholm. *Applied Energy*, 109: 523–529.

Cox SJ, Kim D, Cho H, et al. (2019). Real time optimal control of district cooling system with thermal energy storage using neural networks. *Applied Energy*, 238: 466–480.

Crawley DB, Lawrie LK, Winkelmann FC, et al. (2001). EnergyPlus: creating a new-generation building energy simulation program. *Energy and Buildings*, 33: 319–331.

Deru M, Field K, Studer D, et al. (2011). U.S. Department of Energy Commercial Reference Building Models of the National Building Stock.

Garimella S, Lockyear K, Pharis D, et al. (2022). Realistic pathways to decarbonization of building energy systems. *Joule*, 6: 956–971.

Hou J, Luo X, Huang G, et al. (2020). Development of event-driven optimal control for central air-conditioning systems. *Journal of Building Performance Simulation*, 13: 378–390.

Hu S, Jiang Y, Yan D (2022). China Building Energy Use and Carbon Emission Yearbook 2021: A Roadmap to Carbon Neutrality by 2060. Singapore: Springer Nature.

Huang S, Zuo W, Sohn MD (2016). Amelioration of the cooling load based chiller sequencing control. *Applied Energy*, 168: 204–215.

Huang P, Huang G, Augenbroe G, et al. (2018). Optimal configuration of multiple-chiller plants under cooling load uncertainty for different climate effects and building types. *Energy and Buildings*, 158: 684–697.

Hydeman M, Gillespie KL Jr (2002). Tools and techniques to calibrate electric chiller component models. *ASHRAE Transactions*, 108(1): 733–741.

Kang Y, Jiang Y, Zhang Y (2003). Modeling and experimental study on an innovative passive cooling system—NVP system. *Energy and Buildings*, 35: 417–425.

Kang X, Wang X, An J, et al. (2022). A novel approach of day-ahead cooling load prediction and optimal control for ice-based thermal energy storage (TES) system in commercial buildings. *Energy and Buildings*, 275: 112478.

Kaspar K, Ouf M, Eicker U (2022). A critical review of control schemes for demand-side energy management of building clusters. *Energy and Buildings*, 257: 111731.

Li W, Gong G, Fan H, et al. (2021). A clustering-based approach for "cross-scale" load prediction on building level in HVAC systems. *Applied Energy*, 282: 116223.

Liu Z, Tan H, Luo D, et al. (2017). Optimal chiller sequencing control in an office building considering the variation of chiller maximum cooling capacity. *Energy and Buildings*, 140: 430–442.

Liu Y, Ming H, Luo X, et al. (2023). Timetabling optimization of classrooms and self-study rooms in university teaching buildings based on the building controls virtual test bed platform considering energy efficiency. *Building Simulation*, 16: 263–277.

Lu J, Tian X, Feng C, et al. (2023). Clustering compression-based computation-efficient calibration method for digital twin modeling of HVAC system. *Building Simulation*, 16: 997–1012.

Ma Z, Wang S, Xu X, et al. (2008). A supervisory control strategy for building cooling water systems for practical and real time applications. *Energy Conversion and Management*, 49: 2324–2336.

Miretti F, Misul D, Spessa E (2021). DynaProg: Deterministic Dynamic Programming solver for finite horizon multi-stage decision problems. *SoftwareX*, 14: 100690.

OpenModelica (n.d.). ElectricEIR of Chiller. OpenModelica organization. Available at https://build.openmodelica.org/Documentation/Buildings.Fluid.Chillers.Data.ElectricEIR.html. Accessed 6 Mar 2023.

PCM Products (2024). PCM Products. S10 PCM. Available at https://www.pcmproducts.net

Powell KM, Cole WJ, Ekarika UF, et al. (2013). Optimal chiller loading in a district cooling system with thermal energy storage. *Energy*, 50: 445–453.

Sehar F, Rahman S, Pipattanasomporn M (2012). Impacts of ice storage on electrical energy consumptions in office buildings. *Energy and Buildings*, 51: 255–262.

Seo BM, Lee KH (2016). Detailed analysis on part load ratio characteristics and cooling energy saving of chiller staging in an office building. *Energy and Buildings*, 119: 309–322.

Sun Y, Wang S, Huang G (2009). Chiller sequencing control with enhanced robustness for energy efficient operation. *Energy and Buildings*, 41: 1246–1255.

Tibshirani R, Walther G, Hastie T (2001). Estimating the number of clusters in a data set via the gap statistic. *Journal of the Royal Statistical Society Series B*: *Statistical Methodology*, 63: 411–423.

Wan H, Xu X, Xu T, et al. (2022). Development of a quasi-2D variable resistance–capacitance model for tube-encapsulated phase change material storage tanks. *Applied Thermal Engineering*, 214: 118868.

Woods J, Mahvi A, Goyal A, et al. (2021). Rate capability and Ragone plots for phase change thermal energy storage. *Nature Energy*, 6: 295–302.

Wu R, Ren Y, Tan M, et al. (2024). Fault diagnosis of HVAC system with imbalanced data using multi-scale convolution composite neural network. *Building Simulation*, 17: 371–386.

Xiong Q, Alshehri HM, Monfaredi R, et al. (2022). Application of phase change material in improving trombe wall efficiency: An up-to-date and comprehensive overview. *Energy and Buildings*, 258: 111824.

Yang S, Gao HO, You F (2022). Model predictive control for Demand- and Market-Responsive building energy management by leveraging active latent heat storage. *Applied Energy*, 327: 120054.

Zhang S, Niu J (2016). Two performance indices of TES apparatus: Comparison of MPCM slurry *vs*. stratified water storage tank. *Energy and Buildings*, 127: 512–520.

Zhang Y, Akkurt N, Yuan J, et al. (2020). Study on model uncertainty of water source heat pump and impact on decision making. *Energy and Buildings*, 216: 109950.

Zou W, Sun Y, Gao D, et al. (2023). Globally optimal control of hybrid chilled water plants integrated with small-scale thermal energy storage for energy-efficient operation. *Energy*, 262: 125469.